Vertically stacked temperature disturbances near the equatorial stratopause as seen in cryogenic limb array etalon spectrometer data

AUTHOR(S):

Hayashi, Hiroo; Shiotani, Masato; Gille, John C.

JOURNAL OF GEOPHYSICAL RESEARCH, VOL. 103, NO. D16, PAGES 19,469–19,483, AUGUST 27, 1998

Vertically stacked temperature disturbances near the equatorial stratopause as seen in cryogenic limb array etalon spectrometer data

Hiroo Hayashi and Masato Shiotani
Graduate School of Environmental Earth Science, Hokkaido University, Sapporo, Japan

John C. Gille
National Center for Atmospheric Research, Boulder, Colorado

Abstract. Temperature data derived from the cryogenic limb array etalon spectrometer (CLAES) on board the Upper Atmosphere Research Satellite (UARS) are used to investigate planetary-scale temperature disturbances near the equatorial stratopause for January 1992 to May 1993. The disturbances are characterized by vertically stacked temperature extrema of alternating sign with a vertical scale of about 10 km and have a localized and stationary nature in the longitudinal direction with persistence of about 1 week. These are nearly identical to so-called "pancake structures" first identified by *Hitchman et al.* [1987] using data from the limb infrared monitor of the stratosphere (LIMS). Their analysis suggested that pancake structures are consistent with those predicted by inertial instability theory and that their appearance is synchronized with strong planetary waves in the winter midlatitude, though the LIMS observations were made only during the northern winter. Using the CLAES data for about 14 months, this study shows that pancake structures occur not only during the northern winter but also during the southern winter. In addition, it is found that an equatorial pancake structure has its counterpart with reversed phase in the winter midlatitude, suggesting clear evidence for inertial instability. Further analyses on the basis of Ertel's potential vorticity show that inertially unstable regions intrude locally far into the winter hemisphere around pancake structures that appear when planetary wave breaking is going on. This implies a mechanism of localized inertial instability and resulting pancake structures caused by midlatitude planetary waves in the winter hemisphere, as some numerical studies have inferred.

1. Introduction

Hitchman et al. [1987] (hereafter H87) found a new type of planetary-scale disturbance in the equatorial lower mesosphere during the 1978–1979 northern winter, using data from the limb infrared monitor of the stratosphere (LIMS) on board Nimbus 7 [*Gille and Russell*, 1984]. The disturbances (deviations from the zonal mean) consist of vertically stacked temperature extrema of alternating sign. They have a large amplitude (exceeding 5 K) with a short vertical wavelength (~14 km), are persistent as long as 1 or 2 weeks, and are almost stationary. Owing to their characteristic form, the temperature disturbances were named "pancake structures" in H87.

These pancake structures were anticipated by *Dunkerton* [1981] and *Hunt* [1981], who independently proposed the existence of vertically layered structures in association with inertial instability. *Dunkerton* [1981] theoretically investigated a circulation pattern caused by inertial instability under the zonally symmetric condition and showed that pancake structures would be produced at side boundaries of the unstable region (see Figure 4 in our paper). *Hunt* [1981] found in a perpetual January run of a numerical model of the middle atmosphere that the tropical meridional wind in the northern hemisphere exhibited vertically stacked maxima with alternating signs. He attributed this characteristic feature to inertial instability. *Dunkerton* [1983] extended his previous work to zonally asymmetric modes on a parallel basic flow; furthermore, *Dunkerton* [1993] and *Clark and Haynes* [1996] have investigated inertial instability on a nonparallel basic flow.

The observational analyses by H87 showed that pancake structures appear only when the atmospheric flow is inertially unstable, a condition when there is an imbalance between the pressure gradient and the total centrifugal forces [*Andrews et al.*, 1987]. H87 also found that midlatitude planetary waves are strong when pancake structures are prominent. However, the short lifetime of the LIMS instrument prevented H87 from examining the southern winter.

Another observational work was done by *Fritts et al.* [1992], using the data from mesosphere-stratosphere-troposphere (MST) radar at Jicamarca (12°S, 77°W). They found persistent features in the meridional wind component with vertical scales of 6–10 km in the mesosphere during the southern winter. Though their analysis depends on the one-point ground-based observation, they inferred that the structures are due to inertial instability.

O'Sullivan and Hitchman [1992] followed up on H87 by using a mechanistic middle atmosphere model to investigate the relationship between equatorial inertial instability and midlati-

Paper number 98JD01730.
0148-0227/98/98JD-01730$09.00

tude planetary waves. Their results, as well as subsequent works [e.g., *Dunkerton*, 1993; *Sassi et al.*, 1993; *Clark and Haynes*, 1996], revealed a mutual relationship between localized unstable regions enhanced by planetary waves and divergence/convergence patterns that should represent inertial circulations.

Motivated by these studies, we try to examine whether pancake structures can appear even in the southern winter, though, as is well known, planetary wave activity in the southern hemisphere is relatively weak. To investigate this problem, we make use of data derived from the cryogenic limb array etalon spectrometer (CLAES; refer to *Roche et al.* [1993]) on board the Upper Atmosphere Research Satellite (UARS). CLAES observed the Earth's atmosphere at the limb, and its vertical resolution is good enough to capture pancake structures with vertical wavelength of about 14 km. The period of CLAES data from January 1992 to May 1993 includes two northern winters and one southern winter. In addition, we investigate whether pancake structures are really evidence for inertial instability, and what kind of relationship exists between inertially unstable regions and midlatitude planetary wave activity.

In section 2 we briefly describe the CLAES temperature data and the U.K. Meteorological Office (UKMO) analyses used in this study. In section 3 we show two typical cases of pancake structures, one for the northern winter and the other for the southern winter. Configurations of the potential vorticity field are also discussed for these two cases. In section 4 we examine the activities of pancake structures through the CLAES observation period and compare them with those of midlatitude planetary waves. In section 5 we further introduce supporting evidence that the data from the Halogen Occultation Experiment (HALOE) also observed a similar pancake-like feature. Finally, in section 6 we summarize the present study.

2. Data

2.1. CLAES Data

In this study we use the version 7 (V7) CLAES temperature data. (These results would be essentially unchanged if CLAES V8 temperature data were used.) CLAES was an infrared spectrometer on board the UARS, and a limb-viewing instrument similar to LIMS. (For a general introduction to the UARS mission, see *Reber* [1993].) It measured radiances emitted by the atmosphere over an altitude range from 10–15 km to 60–65 km with a linear array of 20 detectors, each subtending 2.5 km at the limb. Thus the CLAES vertical resolution is good enough to resolve pancake structures which have a vertical wavelength of about 14 km (H87). It sampled vertical profiles 15 times per day at each latitude band, on each ascending (northward) and descending (southward) part of the orbit.

Using a Kalman filter estimation procedure, data are mapped in the form of synoptic coefficients at 1200 UTC during the period of January 9, 1992 to May 5, 1993. Zonal harmonic coefficients (the zonal mean and the cosine and sine coefficients of the first six zonal wavenumbers) are provided at 19 pressure levels with an interval of about 2.5 km, that is, the UARS standard pressure levels defined by $p = 100 \times 10^{-(i-1)/6}$ hPa ($i = 1, 2, \cdots$), and at 4° intervals in latitude from 80°S to 80°N. We averaged the ascending and descending parts.

CLAES alternatively observed from 32°S to 80°N, or 80°S to 32°N, depending on the direction of flight of the UARS spacecraft. It was turned around about every 36 days. In the lower latitude bands (32°S–32°N), however, continuous measurement could be made, so the CLAES data are suitable to study equatorial pancake structures. (For more detailed information on CLAES, see *Roche et al.* [1993] and *Gille et al.* [1996].)

2.2. UKMO Analyses

In order to estimate Ertel's potential vorticity, we use U.K. Meteorological Office analysis data (hereafter UKMO analyses) instead of the CLAES data. The UKMO analyses are global meteorological analyses of the troposphere and stratosphere since October 1991, produced by the technique of data assimilation [*Swinbank and O'Neill*, 1994a]. The analyzed fields are mapped on a 2.5° × 3.75° latitude-longitude grid for 22 pressure levels from 1000 to 0.3 hPa. The pressure levels are decided by $p = 1000 \times 10^{-(i-1)/6}$ hPa ($i = 1, 2, \cdots$), the same as those for CLAES above 100 hPa.

The UKMO analyses are constructed from conventional meteorological measurements in the troposphere and lower stratosphere and nadir-viewing temperature soundings from the National Oceanic and Atmospheric Administration (NOAA) polar-orbiting satellites; they do not include observations from limb-viewing instruments like CLAES. Therefore the UKMO analyses can represent only phenomena whose vertical structures are deep, and they are not good for studying vertically thin structures, such as pancake structures. However, we use the UKMO analyses because they have much better horizontal resolution desirable for calculating potential vorticity, though fine structures would be produced by the model. (For the validation report of UKMO analyses, see *Swinbank and O'Neill* [1994b].)

3. Case Studies

3.1. Pancake Structures

We first try to capture the appearance of equatorial pancake structures as H87 did, which included figures showing time-height sections of the LIMS temperature cosine coefficients for waves 1 and 2. In these figures they paid special attention to characteristic thermal disturbances with vertically stacked extrema in the lower mesosphere. The planetary scale disturbances they found are different from the equatorial Kelvin waves and the midlatitude planetary waves propagating into the equatorial latitude (see Figure 1 in H87).

Figure 1 shows such a time-height section of sine coefficients for wave 1 over the equator as in H87 but based on the CLAES temperature data. The sine coefficients mean wavenumber 1 temperature variations at 90°E longitude, and we can infer the phase information from them. As H87 mentioned that the characteristic disturbances, that is, pancake structures, persist for 1 or 2 weeks, we applied 7-day running means for the data and filtered out shorter-period signals such as due to fast Kelvin waves, but there still remain slow Kelvin waves in the lower stratosphere. In Figure 1 we see some sets of vertically stacked temperature extrema near the stratopause (~1 hPa), during January–February 1992, July–August 1992, and December 1992 to February 1993. These should be indications of pancake structures, and we will confirm their existence further in longitude-height sections of temperature anomalies composed of all wavenumber coefficients. Among them, two typical cases are chosen, one in late July to early August 1992 (a

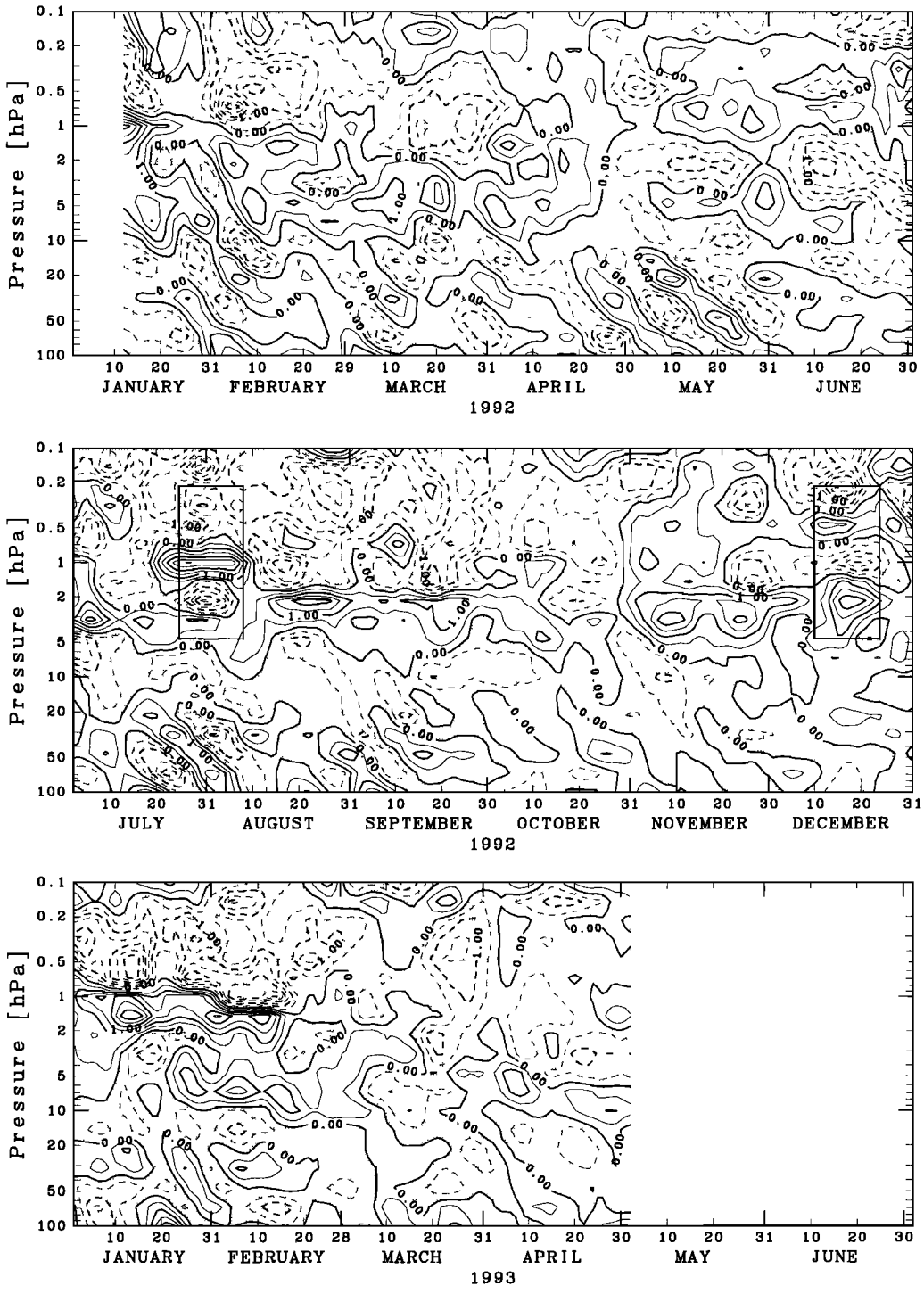

Figure 1. Time-height section of sine coefficients of the CLAES temperature for wave 1. Values are smoothed by 7-day running mean and averaged over the latitude band 4°S–4°N. The shaded regions are negative. Two boxes are centered on August 1, 1992 and on December 17, 1992, with 15-day-period width and about 20 km vertical length (4.6 hPa to 0.2 hPa, including nine pressure levels). The contour interval is 0.5 K.

southern winter case), the other in mid-December 1992 (a northern winter case), marked by the rectangular boxes in Figure 1. The vertical length of each box is about 20 km, extending from the upper stratosphere to the lower mesosphere with a center around the stratopause and 15 day length. In the following we will concentrate on these two cases. Note that CLAES made no observations for a few days when the UARS instrument yawed, but these cases are not coincident with such periods.

Figures 2 and 3 show longitude-height sections of the equatorial temperature anomalies composed of the cosine and sine components of zonal wavenumbers 1–6. We averaged daily

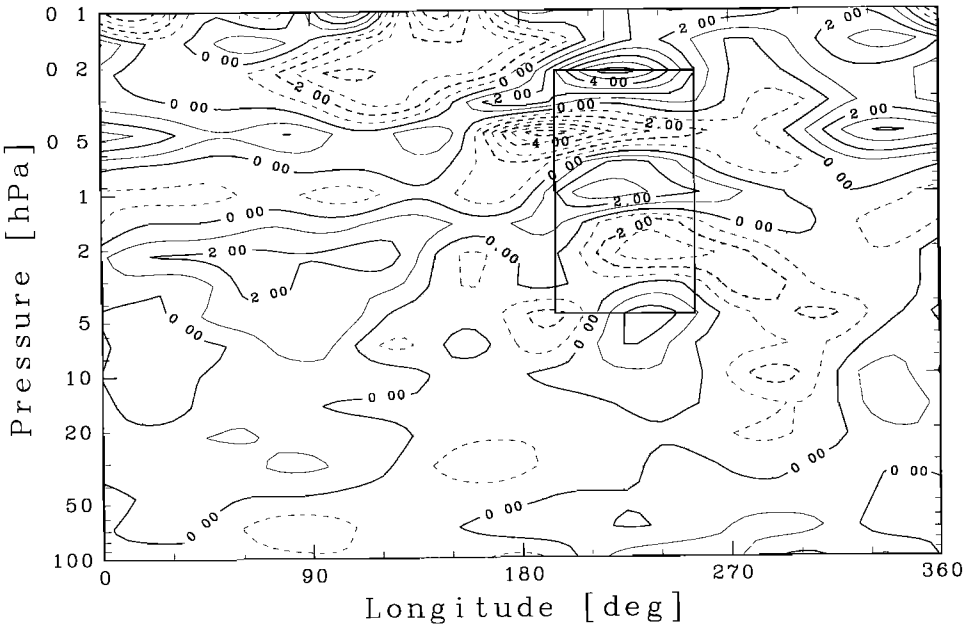

Figure 2. Longitude-height section of the CLAES temperature anomalies at the equator. Values are averaged in the latitude band 4°S–4°N and for 7 days (December 14–20, 1992). All zonal wavenumbers (k = 1–6) are included. Negative values are shaded. The box is centered on 225°E with 60° width and length of 4.6–0.2 hPa. The contour interval is 1 K.

values over 7 days to remove signals with a shorter period and consequently to make pancake structures stand out. In Figure 2, for the northern winter case, as indicated by the box there clearly exists a set of vertically stacked temperature extrema of alternating sign, that is, a pancake structure, centered around 225°E and extending from the upper stratosphere to the lower mesosphere. Its longitudinal structure is not wavelike but localized, which suggests that all wavenumber (1–6) components contribute to the structure. From daily snapshots (not shown) the pancake structure is seen to remain near 225°E for about a week or more, though its amplitude grows and decays. Figure 3 is the same as Figure 2 but for the southern winter case, and a pancake structure is seen near 265°E as indicated by the box. In this case, daily snapshots (not shown) reveal that some parts of the pancake extrema in the lower mesosphere are seen to travel eastward slowly, though the other parts near the stratopause remain at almost the same position. In the lower stratosphere, there appear slow Kelvin wave signals with eastward

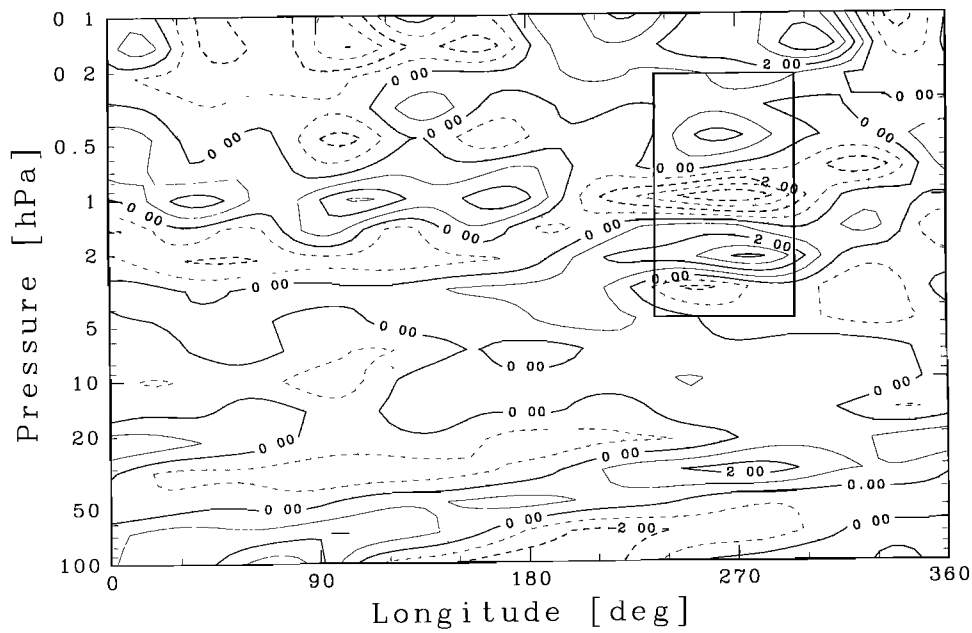

Figure 3. As in Figure 2, except averaged over July 29 to August 4, 1992. The box centered on 265°E is the same size as in Figure 2. The contour interval is 1 K.

phase tilt. Compared with them, the pancake structures have greater amplitudes, over 4 K at the maximum. In daily snapshots the amplitude extrema are as much as 8 K, while those of Kelvin waves are 2–3 K at most [*Shiotani et al.*, 1997].

In both cases the vertical wavelength of pancake structures is about 10 km, which corresponds to the height of five vertical pressure levels and is close to the 14 km of H87 and the 6–10 km of *Fritts et al.* [1992]. Our result is consistent with a theoretical estimate of the vertical scale of pancake structures, which will be mentioned in section 3.3. Moreover, in section 5 we will present additional observations that HALOE on board the UARS also captured similar temperature disturbances with almost the same vertical wavelength. Pancake structures in this study are much more localized than H87 showed, probably because we include all wavenumbers 1–6 to represent the longitudinal structure, whereas H87 used only the first three wavenumbers. Pancake structures in the CLAES temperature have a larger vertical extent, from the upper stratosphere to the lower mesosphere, than those in the LIMS temperature, which existed mainly in the lower mesosphere.

3.2. Evidence for Inertial Instability

H87 stated in their paper that pancake structures were consistent with disturbances predicted by inertial instability theory. Inertial instability is a kind of symmetric instability that redistributes the angular momentum imbalance in a rotating fluid. In the Earth's atmosphere, if we assume zonally symmetric basic flow, a criterion of inertial instability is expressed as

$$f(f - \bar{u}_y) < 0, \tag{1}$$

where f is the Coriolis parameter and $\bar{u}_y$ is the meridional shear of the basic flow [e.g., *Holton*, 1992].

Dunkerton [1981] discussed inertial instability on the equatorial β plane, under an assumption of linear, zonally symmetric perturbations on a zonal mean flow having constant static stability and constant linear shear. He showed that meridional circulations as shown in Figure 4 could arise in unstable regions. Meridional flows indicated by large arrows in Figure 4 induce divergences and convergences at the side boundaries of an inertially unstable area, that is, at latitudes of $f = 0$ and $f = \bar{u}_y$, which lead to vertical motions indicated by small arrows. Then these vertical motions are accompanied by temperature (and geopotential height) extrema, resulting in the pancake structures. From this schematic figure it is supposed that at some latitude away from the equator there is another pancake structure having a reversed phase of the equatorial one. In the following we will clearly show this antiphased pancake structure, which H87 did not show.

Figure 5 shows latitude-height sections of temperature anomalies near 225°E, corresponding to the central longitude of the pancake structure shown in Figure 2 for the northern winter case. In Figure 5a we see the pancake structure over the equator and the large influences of planetary waves in midlatitudes, but there is a fragment of antiphased pancake structure around 20°–30°N. Then we apply a high-pass filter in the vertical direction to the temperature data to reduce influences of planetary waves. The high-pass filter is simply designed by subtracting about 10 km running mean (corresponding to five UARS pressure levels) from the original raw value at each vertical grid point, and consequently we get Figure 5b. This figure indicates that another antiphased pancake structure exists near 30°N, ordinarily hidden by planetary waves with a deep vertical scale. This result strongly supports the concept that pancake structures are caused by inertial instability.

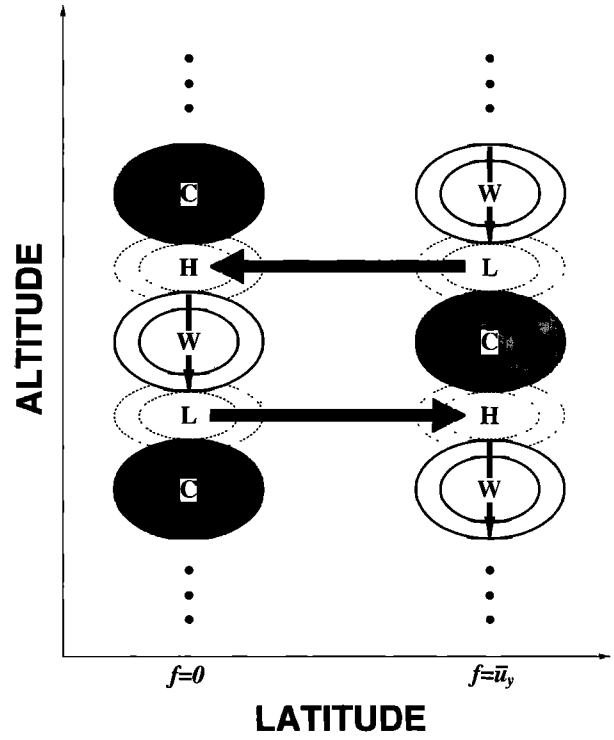

Figure 4. Schematic view of inertial circulations in the meridional plane. W and C are warm and cold anomalies of temperature, while H and L are high and low anomalies of geopotential height. The arrows indicate flows induced by inertial instability (see section 3.2).

Figure 6 shows latitude-height sections of temperature anomalies at 265°E, corresponding to the central longitude of the pancake structure shown in Figure 3 for the southern winter case. The same filtering procedure was performed as in Figure 5; Figure 6a shows raw values and Figure 6b filtered values. In this case we can also recognize another antiphased pancake structure near 35°–40°S, though it is not so clear owing to missing data at high latitudes in the southern hemisphere because of the UARS switch of the viewing directions. This result in the southern winter case gives us further confidence that pancake structures are due to inertial instability.

Using this high-pass filter approach for the LIMS data, we could find antiphased pancake structures in the midlatitude (J. A. Knox, personal communication, 1998).

3.3. Vertical Scale

As shown in Figures 2–6, the typical vertical scale of pancake structures is estimated to be about 10 km. H87 estimated 14 km as its vertical scale and presented the validity by comparing with the theoretical estimates. Here we also examine whether our observational result of vertical scale (~10 km) is consistent with the theory.

Dunkerton [1981] assumed eddy diffusivity to get a finite vertical scale of unstable mode. Indeed, H87 and *Fritts et al.* [1992] estimated a vertical scale with a value of diffusivity predicted by gravity wave breaking, though it is not accurately known. Here we use another theoretical estimate, which was introduced by H87.

Assuming small–zonal wavenumber inertial waves and set-

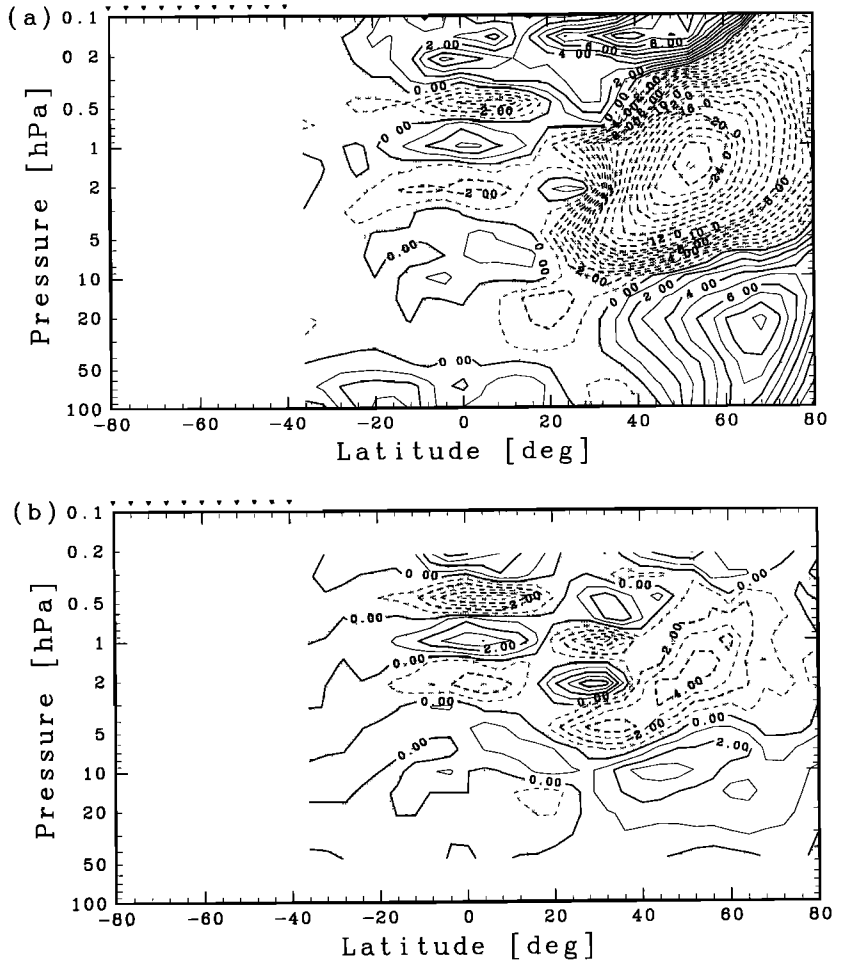

Figure 5. Latitude-height sections of the CLAES temperature anomalies (k = 1–6). (a) Values are averaged for 7 days (December 14–20, 1992) and over 60° longitudinal width centered on 225°E, corresponding to the center of the pancake structure shown in Figure 2. The contour interval is 1 K ($|T| \leq 10$ K) and 2 K ($|T| > 10$ K). (b) Filtered values of Figure 5a with use of the high-pass filter (see text). The contour interval is the same as in Figure 5a.

ting frequency to be zero, we obtain the relationship between vertical wavelength (L_z) and meridional wavelength (L_y) equated as

$$L_z = \frac{\pi}{4}\frac{\gamma}{N} L_y, \tag{2}$$

where γ and N are static stability and meridional shear $\bar{u}_y$, respectively (see equations (6.4)–(6.6) in H87). Note that we suppose zero frequency because pancake structures are synchronized with quasi-stationary planetary waves in the midlatitude as will be shown in sections 3.4 and 4.

From results of the two case studies we knew that equatorial pancake structures have their counterparts in 30°–40° latitude, so we take $L_y/2$ = 3300–4400 km. On the other hand, we estimate γ from the UKMO analyses as the average of meridional shear between 5° and 30° latitude, around central longitudes of the pancake structures. Although the value has large day-to-day variability, we estimate it to be 2–4 × 10^{-5} s^{-1} when pancake structures appear. Then taking N = 0.02 s^{-1}, a vertical scale of pancake structures is estimated in the range of 5–14 km. This result supports observational estimate (~10 km), though there remains an essential problem, whether relationship (2) based on the assumption of small zonal wavenumber can apply to these extremely localized cases.

3.4. Background Conditions

Considering linear inertial instability theory under the assumption that small parcel excursions never change the mass distribution, inertially unstable regions with zonal symmetry are expressed by the criterion of (1). In this case, however, the estimation of inertially unstable regions based on the zonal mean wind field never exceeds 20° in the latitudinal direction (not shown), while the meridional scale of pancake structures reaches 30°–40° and pancake structures are very local, as shown in Figures 2 and 3. This fact suggested that the zonal mean assumption is not satisfied during pancake episodes.

Generalizing this criterion, *O'Sullivan and Hitchman* [1992] pointed out that a parcel displaced horizontally a distance δs perpendicular to the regional large-scale velocity vector will be accelerated at the rate

$$\frac{\partial^2 \delta s}{\partial t^2} = -f(f + \zeta)\, \delta s, \tag{3}$$

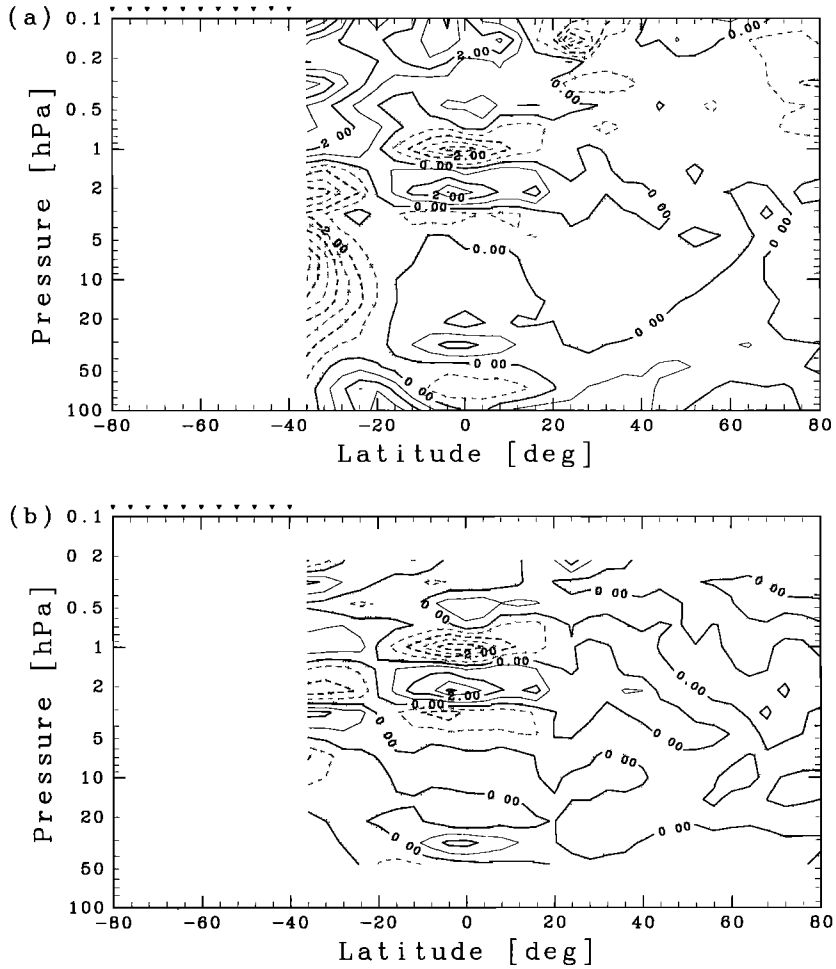

Figure 6. As in Figure 5. (a) Values are averaged for 7 days (July 29 to August 4, 1992) and over 60° longitudinal width centered on 265°E, corresponding to the center of the pancake structure shown in Figure 3. The contour interval is 1 K ($|T| \leq 10$ K) and 2 K ($|T| > 10$ K). (b) Filtered values of Figure 6a with use of the high-pass filter. The contour interval is the same as in Figure 6a.

where $\zeta = \partial v/\partial x - \partial u/\partial y$ is the relative vorticity. Therefore the generalized criterion of inertial instability is represented by

$$f(f + \zeta) < 0. \tag{4}$$

On the other hand, Ertel's potential vorticity (EPV) on an isentropic surface is written as

$$P = -g(f + \zeta)\frac{\partial \theta}{\partial p} \tag{5}$$

where P, g, θ, and p are EPV, gravity, potential temperature, and pressure, respectively [*Hoskins et al.*, 1985]. From (4) and (5), inertial instability is expected to occur where EPV values are negative (positive) in the northern (southern) hemisphere. In the following, such EPV values with the opposite sign to that expected for values in each hemisphere are referred as "anomalous EPV."

O'Sullivan and Hitchman [1992] used a mechanistic model of the middle atmosphere to show that strong divergence/convergence patterns, that is, the regions of inertial circulations, approximately correspond to anomalous EPV regions; they are locally pulled across the equator far into the midlatitude in the winter hemisphere by the influences of midlatitude planetary waves (see Figure 9 in their paper, for example). *Sassi et al.* [1993], in their numerical study on the stratopause semiannual oscillation, also showed a similar result of good agreement between the regions of inertial circulations and localized anomalous EPV when strong planetary waves appear in the winter hemisphere. *Dunkerton* [1993] studied the growth of inertially unstable modes in nonparallel flow on an equatorial β plane by use of a simple two-dimensional model. His results suggested that it is possible for local and stationary modes of inertial instability to appear. All these investigations imply an intimate relationship among localized inertial circulations, anomalous EPV regions (i.e., regions expected to be inertially unstable), and midlatitude planetary waves. Next, we examine EPV distributions for the two foregoing cases of pancake structures.

Figures 7 and 8 show series of EPV maps with the horizontal wind fields on an isentropic surface near the stratopause, on a 1850 K surface (~1.0 hPa), with use of the polar stereographic projection. These figures include three typical stages: (1) when the pancake structure shown in Figure 2 or 3 begins to be recognized (the initial stage), (2) when it has developed to have maximum amplitudes (the mature stage), and (3) when it almost disappears (the final stage). The outer circle in these figures indicates the equator, the lightly shaded area is for

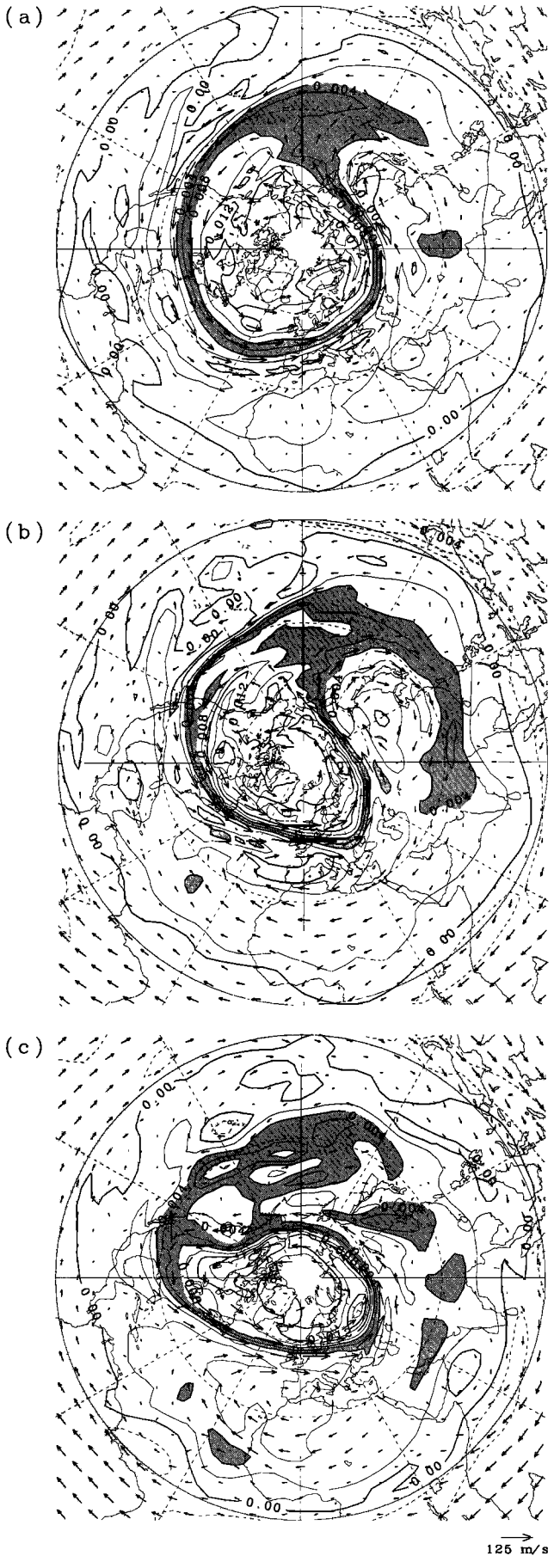

negative (positive) EPV in the northern (southern) hemisphere, and the heavily shaded area is for typical EPV values at midlatitudes close to the vortex edge. Since EPV fields are calculated from the UKMO analyses as mentioned in section 2, we should keep in mind that Figures 7 and 8 only represent vertically deep structures.

Figure 7 is for the case of the northern winter. On December 13 (Figure 7a), some parts of heavily shaded regions are pulled westward and equatorward around 150°–180°E, which causes winter westerlies to be distorted; on the western longitude of the region, flows are almost southward, while on the eastern longitude they are northeastward. Then anomalous EPV (negative EPV) regions are pulled across the equator into the northern hemisphere around 180°E. On December 17 (Figure 7b), the heavily shaded regions have been largely stretched and folded and form a "comma" shape, which means the planetary wave breaking is about to occur. Anomalous EPV regions intrude so much further that some of them reach over 30°N around 210°E. Then the wind field is extremely deformed; easterlies occupy wide regions from 300°E (60°W) to 150°E, extending across the equator to 30°N, while in the opposite longitudes (180°E–270°E), strong westerlies shift to the lower latitudes to make a meridional shear large enough to satisfy the inertial instability condition (4). On December 21 (Figure 7c), some separations of high-EPV blobs (heavily shaded regions) are seen, indicating the planetary wave breaking is occurring. The large intrusion of anomalous EPV regions mostly disappears. Although easterlies remain in the lower latitudes, the wind field seems to be returning to a winter westerly circulation. All these background states are consistent with the space and time development of the pancake structure observed around 225°E having its counterpart in 30°N during the same period (Figures 2 and 5).

A similar situation is seen in Figure 8 for the case of the southern winter pancake structure. On July 29 (Figure 8a), distorted heavily shaded regions imply that the planetary wave has fully developed. It is seen in 180°–270°E that the anomalous EPV (positive EPV) regions are pulled into the winter hemisphere. The wind field is, of course, distorted; strong winter westerlies move toward the equator in 180°–270°E, while easterlies extend to 30°S in 0°E–150°E. On August 1 (Figure 8b) the planetary wave breaking is going on, with many EPV blobs (heavily shaded regions). Then strong westerlies in the lower latitude produce a large meridional shear satisfying the unstable condition, resulting in localized intrusion of the anomalous EPV regions around 240°E with southeastward extension reaching 30°S at 270°E. On August 4 (Figure 8c), though small EPV blobs are still left, the wave breaking event has ended, and the large intrusion of anomalous EPV regions is never seen. The wind field mostly recovers zonal westerlies in the midlatitude with weak zonal easterlies in the lower latitude.

Figure 7. (Opposite) Polar stereographic maps of Ertel's potential vorticity on 1850 K isentropic surface (near 1.0 hPa) on (a) December 13, (b) December 17, and (c) December 21, 1992. The contour interval is 0.002 K m^2 kg^{-1} s^{-1}. The outer circle (solid) is the equator, the inner circles (dashed) correspond to 30°N and 60°N. The longitude increases counterclockwise with Greenwich meridian at the bottom. The lightly shaded regions are negative EPV, while the heavily shaded regions are between 0.004 and 0.008 K m^2 kg^{-1} s^{-1}. The arrows indicate wind vectors.

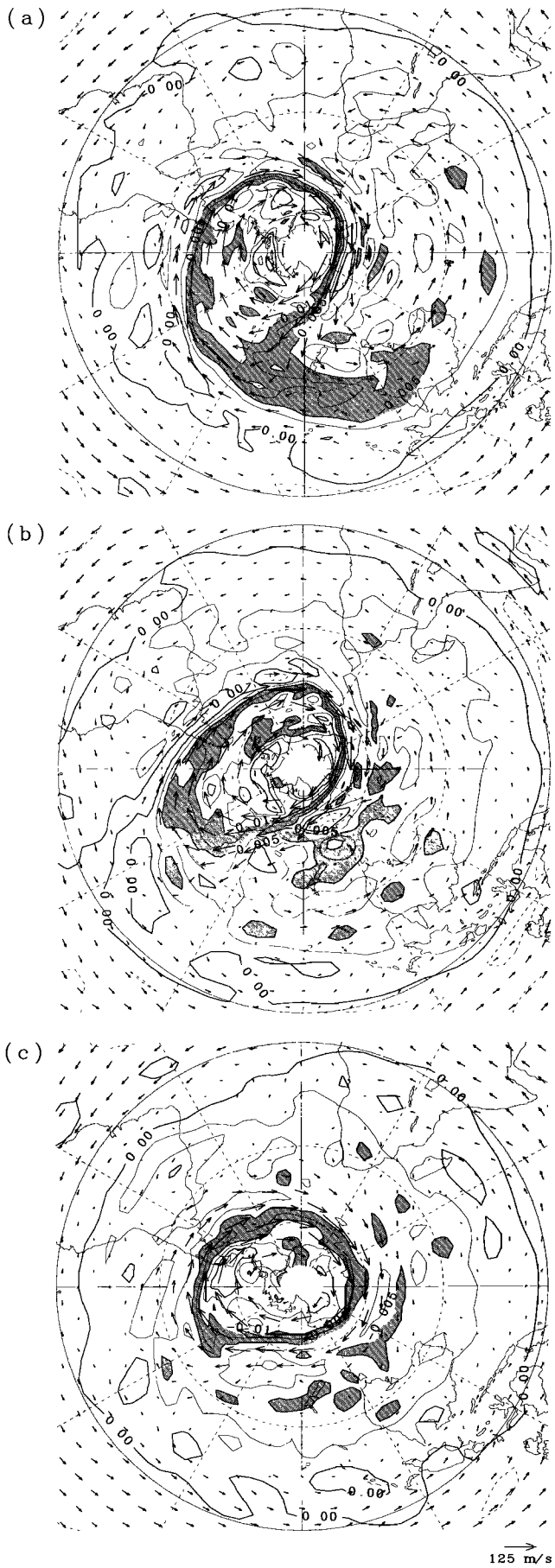

These background states must be desirable for the pancake structures shown in Figures 3 and 6.

4. A Climatology of Pancake Structures for the CLAES Period

So far, we have investigated only two representative cases in the northern and the southern winters. Here we try to infer activity of pancake structures around the equatorial stratopause for the whole CLAES observation period. As seen in the previous section, pancake structures extend from the upper stratosphere to the lower mesosphere with a short vertical wavelength (~10 km) and appear locally confined in longitude. On the basis of these facts, we calculated a variance over the height range 4.6–0.2 hPa (including nine CLAES pressure levels centered at 1 hPa and corresponding to about 20 km) at every longitude (10° interval) and every observation day. Note that before calculating variances the data are smoothed by the use of a 7-day running mean to remove the high-frequency variability such as that due to fast Kelvin waves and are filtered vertically by the high-pass filter mentioned in section 3.2 to remove the vertically deep structures such as those due to planetary waves. If there exist pancake structures, variances should be large. Then, we define the activity of pancake structures as variances calculated according to the above.

Figure 9 shows time-longitude sections of CLAES temperature variances over the equator, that is, indices of equatorial pancake structure activity. Shaded regions in Figure 9 indicate appearances of pancake structures. Although CLAES observed only two northern winters and one southern winter, it is clear that active periods of pancake structures are seen two or three times during each winter season for both hemispheres. Among the large variances corresponding to pancake structures, some are stationary at a certain longitude (in late June to early July 1992 and mid-December 1992); others travel slightly eastward (in late July to early August 1992 and late January to early February 1993). There is a case when two pancake structures occur simultaneously at different longitudes (in mid-January 1993). The pancake episode of mid-January 1992, though the data capture only the decaying stage, would be related to the inertial circulation found by *Orsolini et al.* [1997] using UKMO analyses.

In midlatitudes, on the other hand, we investigate planetary wave activity. In this case we calculated temperature anomalies averaged over the same height range as in Figure 9. Usually, planetary waves at midlatitudes have a long vertical wavelength (exceeding 20 km), so the averaging procedure used here makes them clear when they have large amplitudes. In addition, because these planetary waves are associated with asymmetric outflow of cold air in the polar vortex toward lower latitudes, the planetary wave activity should be characterized by localized large negative values. Figure 10 shows time-longitude sections of vertically averaged temperature anomalies, that is, indices of planetary wave activity, in the winter

Figure 8. (Opposite) As in Figure 7, except for on (a) July 29, (b) August 1, and (c) August 4, 1992. The contour interval is 0.0025 K m^2 kg^{-1} s^{-1}. In this case the inner circles (dashed) correspond to 30°S and 60°S, and the longitude increases clockwise with Greenwich meridian at the top. The lightly shaded regions are positive EPV, while the heavily shaded regions between −0.005 and −0.01 K m^2 kg^{-1} s^{-1}.

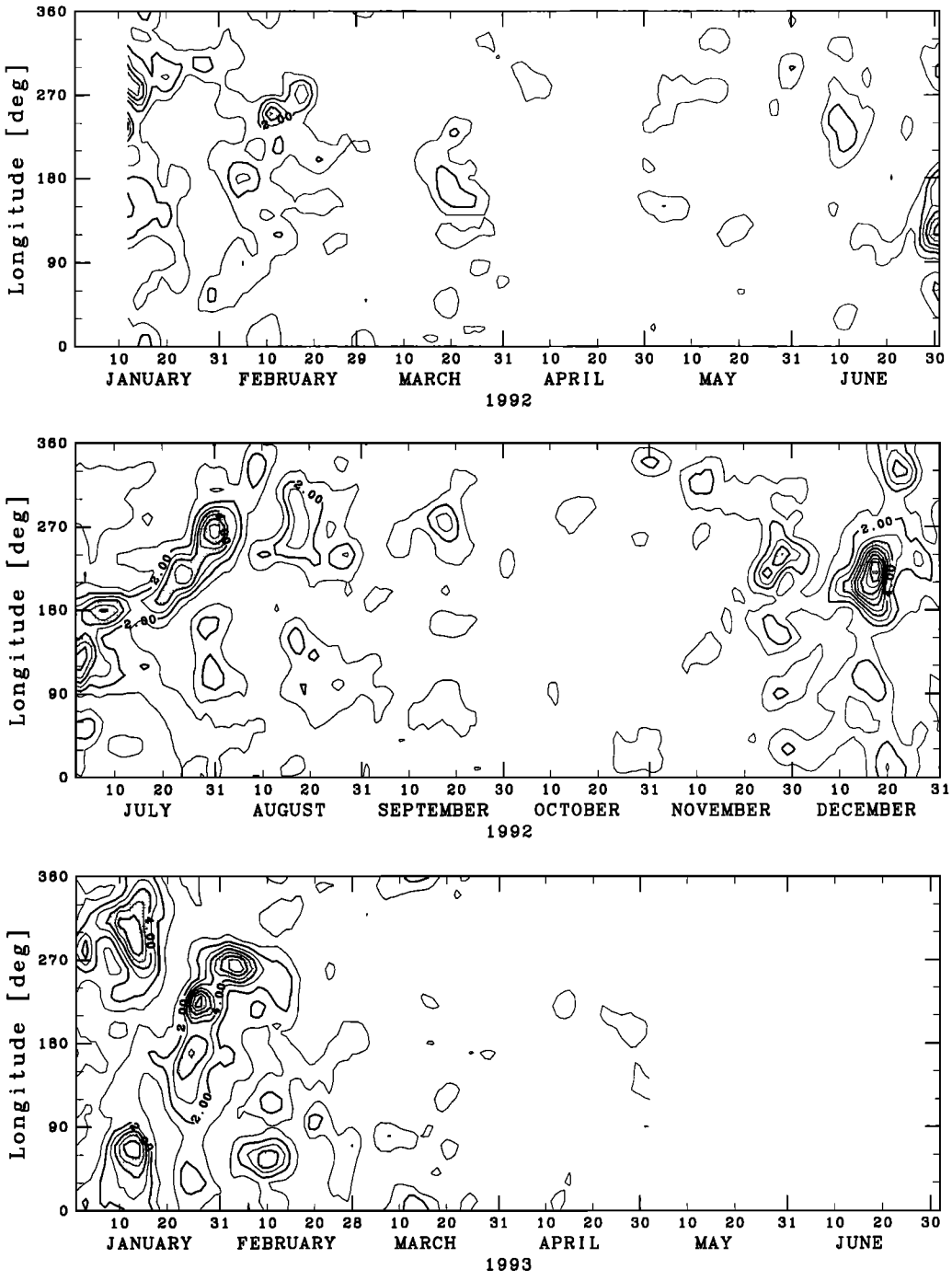

Figure 9. Time-longitude section of CLAES temperature variances between 4.6 and 0.2 hPa (including nine pressure levels). All zonal wavenumbers (k = 1–6) are included. Values are averaged over the latitude band 4°S–4°N, smoothed by taking the 7-day running mean, and filtered with use of the high-pass filter. The regions over 4 K are shaded. The contour interval is 1 K.

midlatitude averaged over 24°–36°N during October to March and over 24°–36°S during April to September. For consistency, the data are smoothed by the use of a 7-day running mean. Shaded regions in Figure 10 indicate strong planetary waves and eventually wave breaking events. There are two or three times when planetary waves are highly active, similar to equatorial pancake structures. From daily snapshots of the EPV map (not shown), localized intrusion events of anomalous EPV regions are confirmed during these periods.

Compared with Figure 9, it is clear that active periods of equatorial pancake structures almost correspond to (or are slightly preceded by) those of planetary waves at midlatitudes in the winter hemisphere, though there is an exception for such a case in mid-January 1993. It is also seen that locations of vigorous pancake structures are always on the eastern side of localized negative anomalies of planetary waves. This is consistent with the case studies in which inertially unstable regions appeared on the eastern side of

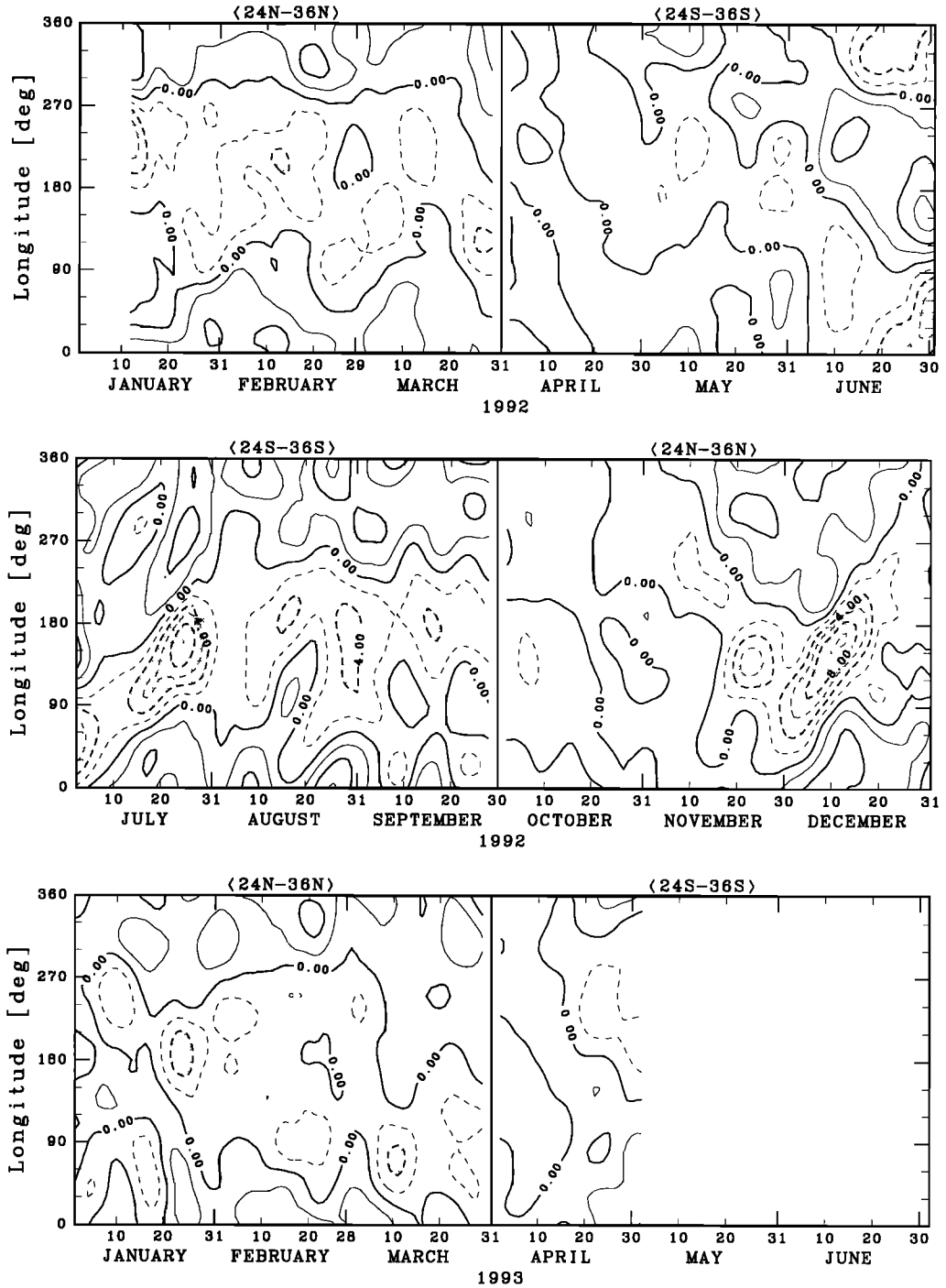

Figure 10. Time-longitude section of the CLAES temperature anomalies (k = 1–6). Values are averaged vertically between 4.6 and 0.2 hPa, and over the latitude band 24°–36°N (between October and March) or 24°–36°S (between April and September). They are also smoothed by taking the 7-day running mean. The regions below −4 K are shaded. The contour interval is 2 K.

the EPV tongue drawn from the winter midlatitude during the planetary wave developing or breaking events (see Figures 7 and 8).

5. Pancake Structures in the HALOE Data

In order to acquire confidence in the existence of pancake structures in the CLAES temperature data, we will show some comparisons between the CLAES and the HALOE data when pancake structures appear.

HALOE is another of the instruments on board the UARS. (For detailed information on HALOE, see *Russell et al.* [1993] and *Hervig et al.* [1996].) We use the version 18 HALOE temperature and ozone mixing ratio data. HALOE observed the atmosphere using a solar occultation technique, 15 times a day along the latitude band for both the ascending part and the

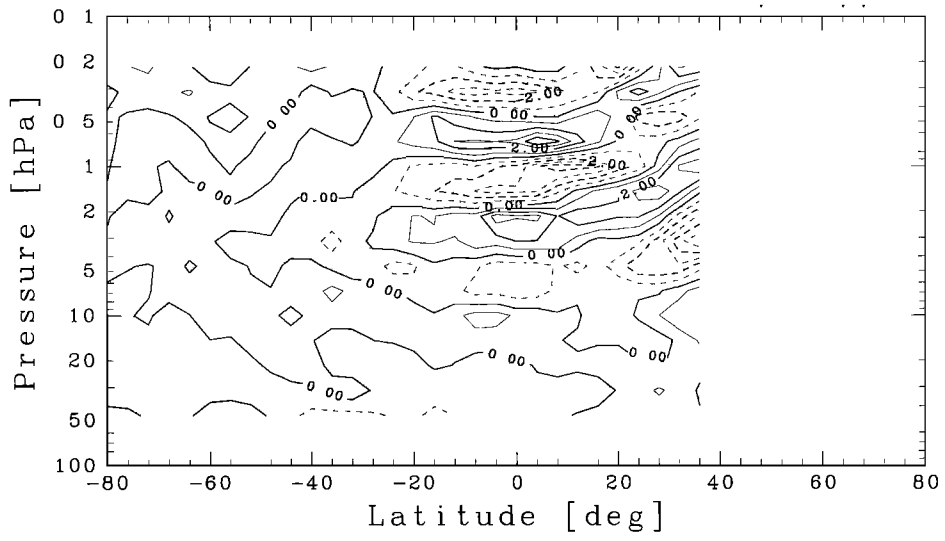

Figure 11. Latitude-height sections of the CLAES temperature anomalies (k = 1–6). Values are averaged for 7 days (January 24–30, 1993) and over 60° longitudinal width centered on 225°E, and filtered with use of the high-pass filter. The contour interval is 1 K.

descending part of the orbit. Its vertical field of view is 1.6 km [*Russell et al.*, 1993], so the HALOE has better vertical resolution than the CLAES. Note that because of aerosol effects in the middle and lower stratosphere, the temperature profiles from 35 to 45 km are formed using a weighted transition from retrieved results to National Meteorological Center (NMC) temperatures, and those below 35 km are completely replaced by NMC.

Figure 11 shows a latitude-height section of the CLAES temperature around 225°E, averaged for 7 days and filtered with the same high-pass filter as used in Figures 5 and 6. Pancake structures are recognized at the equator and around 35°N, though the midlatitude one is not clear since data poleward of 40°N are missing. Around the same days, there are coincidences of the HALOE observation at equatorial latitudes (ascending part) and at winter midlatitudes (descending part). In the following we will compare the CLAES temperature data at 225°E with the HALOE temperature profiles around this longitude.

Figure 12 shows a comparison between a HALOE profile near the equatorial pancake structure with its zonal mean profile, where zonal mean values are estimated by averaging 15 profiles centered around it. The vertical profile at this point (solid line) fluctuates around the zonal mean profile (dashed line) at intervals of about 10 km near the stratopause, so we expect the anomaly, that is, the deviation from the zonal mean, would have a wavelike profile corresponding to the pancake structure. A profile near the midlatitude pancake structure also represents similar fluctuations to those at the equator (not shown).

Then we estimate deviations from zonal mean and compare them with the CLAES temperature anomalies (including zonal wavenumbers 1–6), as shown in Figure 13. The left-hand side of Figure 13 is for the equatorial pancake structure, and the right-hand side for the midlatitude. Influences from planetary waves are removed by the high-pass filter as used in Figures 5 and 6. Although there are some disagreements in amplitude, the fluctuating patterns are very similar between HALOE and CLAES, particularly in the upper stratosphere and the lower mesosphere. In addition, if we compare the left figure (equator) with the right (midlatitude), the two temperature profiles are in opposite phase with each other. Thus Figure 13 enhances our confidence in the CLAES data and the existence of pancake structures.

In addition, we investigate the HALOE ozone data to ascertain the validity of the HALOE temperature data. *Hirota et al.* [1991] described in their paper that the variations of ozone mixing ratio and temperature are strongly negatively correlated in the middle and upper stratosphere. Around this height range they showed the relation between ozone and tempera-

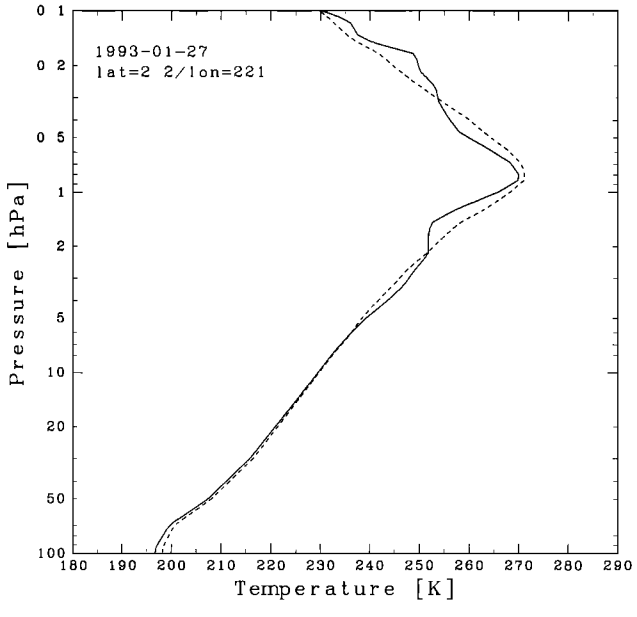

Figure 12. Vertical profiles of the HALOE temperature at 221°E, 2.2°N on January 27, 1993 (solid line), and the zonal mean in the latitude band around 2.2°N, estimated from 15 profiles centered around it (dashed line).

ture is written (using reaction rates from *Watson et al.* [1988]), in differential form, as

$$\frac{d\mu_e}{\mu_e} = \left(-\frac{1030}{T^2} - \frac{1.15}{T} \right) dT \sim -0.02\, dT, \qquad (6)$$

where μ_e and T are ozone mixing ratio at photochemical equilibrium and temperature, respectively, and the right-hand term was approximated by assuming $T \sim 260$ K. Here we consider μ_e as zonal mean and $d\mu_e$ as deviation from it. We compare temperature anomalies and ozone anomalies near the equatorial pancake structure in Figure 14, where the ozone anomaly is normalized by the zonal mean and multiplied by -50. Values are filtered with the high-pass filter. Figure 14 shows that the ozone mixing ratio also has a disturbance with a vertical wavelength of 10 km and gives good agreement with the temperature anomaly near the stratopause. Thus Figure 14 proves mutual reliability of the HALOE temperature and ozone data.

6. Summary

Using global temperature data from the CLAES on board the UARS, we have investigated characteristic disturbances of the temperature field near the equatorial stratopause, so-called, "pancake structures," which were first identified in the LIMS data by *Hitchman et al.* [1987] (H87). Through the present study some new evidence concerning these structures has been obtained. Using CLAES data throughout its observation period (January 1992 to May 1993), we found that pancake structures appear two or three times, not only during the northern winter, but also during the southern winter. In case studies we showed clear pancake structures extending from the upper stratosphere to the lower mesosphere over the equator. They are not wavelike, but highly localized in the longitudinal direction. The typical vertical scale of pancake structures is estimated as about 10 km, which is consistent with a theoretical estimate. As mentioned in section 5, the existence of pancake structures with this scale is confirmed using an independent data set from the HALOE experiment.

We found clear evidence that pancake structures could be understood as results of inertial instability. With the use of a simple high-pass filter, we made it clear that a pancake structure over the equator has its counterpart with the opposite phase in the winter midlatitude, which is very similar to the theoretical expectation by *Dunkerton* [1981]. The antiphased pancake structures are masked by planetary waves in the midlatitude with their vertically deep structure.

Using UKMO analyses we calculated Ertel's potential vorticity (EPV) fields in order to examine the background states when pancake structures appear. As H87 and some numerical studies [*O'Sullivan and Hitchman*, 1992; *Dunkerton*, 1993; *Sassi et al.*, 1993; *Clark and Haynes*, 1996] linked pancake structures or localized inertial instability to the forcing of midlatitude planetary waves, our results exhibit localized intrusions of anomalous EPV regions when planetary wave breaking occurs. The area of anomalous EPV roughly corresponds to regions in which pancake structures exist. Furthermore, from Figures 9 and 10 it was shown that the active period of pancake structures occurs a little later than that of planetary waves, and pancake structures are located on the eastern side of negative maxima of planetary waves.

On the basis of these results, we infer the relationship among pancake structures, inertial instability, and planetary waves, as depicted in Figure 15. This schematic picture shows

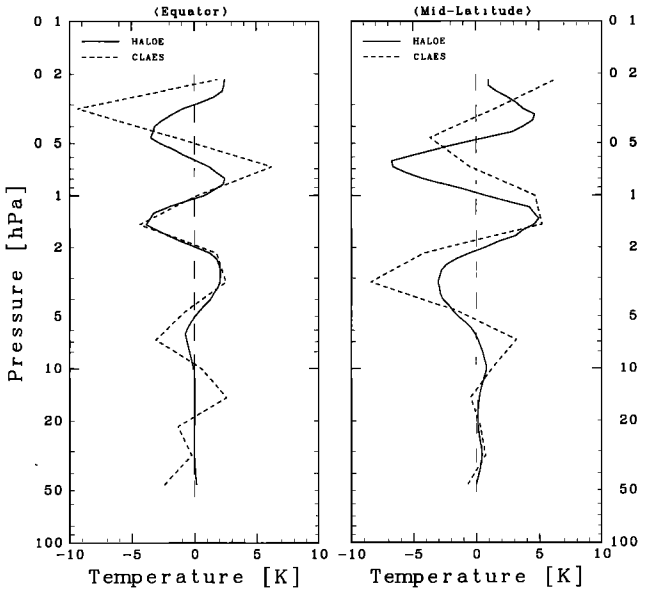

Figure 13. Comparisons between the HALOE temperature anomalies (solid) and the CLAES temperature anomalies (dashed) near the equator (left) and near 35°N (right), around the days when the pancake structures appear. Values are filtered by the high-pass filter. The HALOE profile near the equator is at 221°E, 2.2°N on January 27, 1993, and that near 35°N is at 227°E, 34.3°N on January 28, 1993. The CLAES temperature near the equator is estimated for 225°E, 0°N on January 27, 1993, and that near 35°N is estimated for 225°E, 32°N on January 28, 1993.

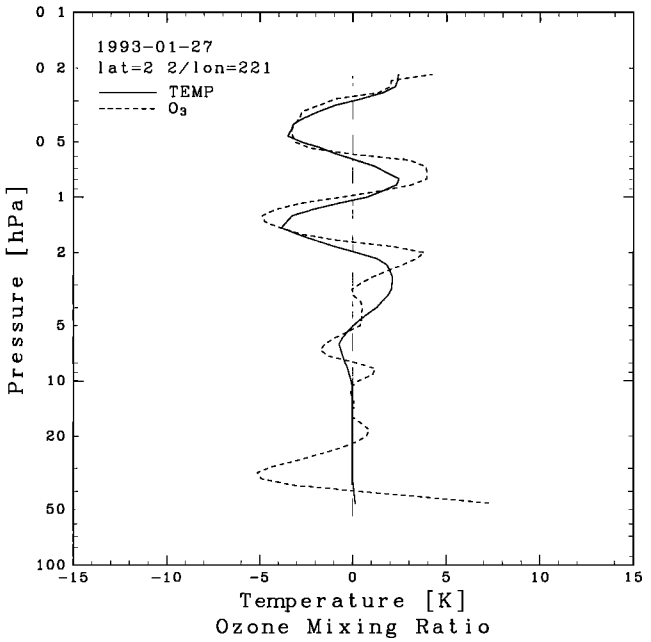

Figure 14. Comparison between the HALOE temperature anomalies (solid) and the HALOE ozone mixing ratio anomalies (dashed) near the equator. Both profiles are for 221°E, 2.2°N on January 27, 1993, and filtered by the high-pass filter. Ozone data are normalized by the zonal mean and multiplied by -50 (see text).

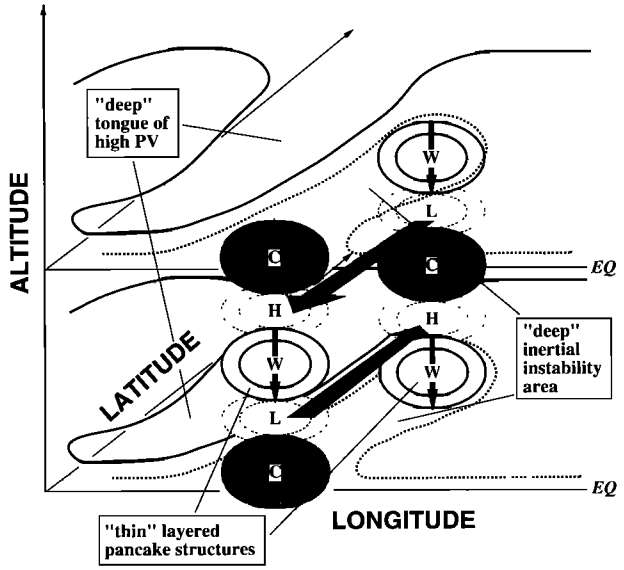

Figure 15. Schematic view of the relationship among pancake structures, inertial instability, and planetary waves in the northern hemisphere. The solid contours mean high-EPV tongue due to the breaking event of planetary waves, while the area between the dashed contour and the equator means anomalous EPV, that is, inertially unstable regions. The symbols and arrows in the pancake structures are the same as in Figure 4.

their relationship for the northern winter case; pancake structures appear as "thin" layered structures embodied in "deep" inertially unstable regions which planetary wave development has made localized on the eastern side of the "deep" high-EPV tongue. Extension of the high-EPV tongue and localized intrusion of inertially unstable regions should be important for material transport between the polar region and equatorial latitudes. In our preliminary investigation of the CLAES N_2O mixing ratio field, we found that N_2O distribution patterns are essentially similar to Figures 7 and 8. *Knox* [1996] also showed using N_2O data from the improved stratospheric and mesospheric sounder (ISAMS) on board the UARS that there exists a localized transport from the tropics to the midlatitude in an episode of inertial instability in the lower stratosphere. Moreover, we believe that vertically thin meridional circulations which consequently make pancake structures play a role of rapid mixing to homogenize EPV in the subtropics.

In this study our analyses with the CLAES data are restricted to the temperature field. We also estimated horizontal winds from the geopotential height data on the basis of "balance winds" introduced by H87. Latitude-height sections of the zonal mean zonal wind showed that penetration of the summer easterlies into the winter hemisphere near the stratopause is halted and reversed when pancake structures appear (not shown). This is consistent with an inference that inertial circulation should contribute to reduction of the meridional shear to restore inertially stable conditions. However, the anomaly wind field from the zonal mean was less correlated with the flow structure expected from inertial instability theory (Figure 4). We need much more careful treatment of the flow field near the equator, and such investigations should be done using the wind data directly measured by the high-quality ground-based or satellite observations.

During the winter of the northern and southern hemispheres, pancake structures tend to appear because the semi-annual oscillation (SAO) around the equatorial stratopause is dominated by the strong easterlies, which leads to inertially unstable conditions in the winter subtropics. Thus seasonal and interannual variability in the SAO easterly regime should be expected to affect the general characteristics of pancake structures, for example, appearance frequency, preferred longitude, and asymmetry between the two hemispheres, though in the present study distinct differences between pancake structures in the northern and southern winters are not clear.

We have discussed pancake structures in association with inertial instability, based on our finding of antiphased pancake structures in the midlatitude expected by theory [*Dunkerton*, 1981]. However, there remains a question as to whether they can really be explained by inertial instability theory alone. Some theoretical works [e.g., *Dunkerton*, 1990; *Winter and Schmitz*, 1998] infer that "divergent barotropic instability" also could produce unstable waves with a similar latitudinal pattern, that is, a set of the equatorial and subtropical maxima which are out of phase to one another. Pancake structures in this study may be related to this instability.

Acknowledgments. We would especially like to thank John A. Knox for his critical comments and valuable suggestions on the original version of this paper. Helpful comments of three anonymous reviewers are also acknowledged. We acknowledge the U.K. Meteorological Office and the HALOE science team for providing the data sets and Nozomi Kawamoto for handling the HALOE data. Most graphical outputs were made by use of the GFD-DENNOU Library. This work was supported in part by the Grant-in-Aid for Scientific Research, the Ministry of Education, Science, and Culture of Japan. Work by J.C.G was supported by the National Aeronautics and Space Administration under Interagency Agreement S-10782. The National Center for Atmospheric Research is sponsored by the National Science Foundation.

References

Andrews, D. G., J. R. Holton, and C. B. Leovy, *Middle Atmosphere Dynamics*. 489 pp., Academic, San Diego, Calif., 1987.

Clark, P. D., and P. H. Haynes, Inertial instability on an asymmetric low-latitude flow, *Q. J. R. Meteorol. Soc.*, *122*, 151–182, 1996.

Dunkerton, T. J., On the inertial stability of the equatorial middle atmosphere, *J. Atmos. Sci.*, *38*, 2354–2364, 1981.

Dunkerton, T. J., A nonsymmetric equatorial instability, *J. Atmos. Sci.*, *40*, 807–813, 1983.

Dunkerton, T. J., Eigenfrequencies and horizontal structure of divergent barotropic instability originating in tropical latitudes, *J. Atmos. Sci.*, *47*, 1288–1301, 1990.

Dunkerton, T. J., Inertial instability of nonparallel flow on an equatorial β plane, *J. Atmos. Sci.*, *50*, 2744–2758, 1993.

Fritts, D. C., L. Yuan, M. H. Hitchman, L. Coy, E. Kudeki, and R. F. Woodman, Dynamics of the equatorial mesosphere observed using the Jicamarca MST radar during June and August 1987, *J. Atmos. Sci.*, *49*, 2353–2371, 1992.

Gille, J. C., and J. M. Russell III, The limb infrared monitor of the stratosphere: Experiment description, performance, and results, *J. Geophys. Res.*, *89*, 5125–5140, 1984.

Gille, J. C., et al., Accuracy and precision of cryogenic limb array etalon spectrometer (CLAES) temperature retrievals, *J. Geophys. Res.*, *101*, 9583–9601, 1996.

Hervig, M. E., et al., Validation of temperature measurements from the Halogen Occultation Experiment, *J. Geophys. Res.*, *101*, 10,277–10,285, 1996.

Hirota, I., M. Shiotani, T. Sakurai, and J. C. Gille, Kelvin waves near the equatorial stratopause as seen in SBUV ozone data, *J. Meteorol. Soc. Jpn.*, *69*, 179–186, 1991.

Hitchman, M. H., C. B. Leovy, J. C. Gille, and P. L. Bailey, Quasi-stationary zonally asymmetric circulations in the equatorial lower mesosphere, *J. Atmos. Sci.*, *44*, 2219–2236, 1987.

Holton, J. R., *An Introduction to Dynamic Meteorology*, 511 pp., Academic, San Diego, Calif., 1992.

Hoskins, B. J., M. E. McIntyre, and A. W. Robertson, On the use and significance of isentropic potential vorticity maps, *Q. J. R. Meteorol. Soc.*, *111*, 877–946, 1985.

Hunt, B. G., The maintenance of the zonal mean state of the upper atmosphere as represented in a three-dimensional general circulation model extending to 100 km, *J. Atmos. Sci.*, *38*, 2172–2186, 1981.

Knox, J. A., A *theoretical and observational study of inertial instability and nonlinear balance*, Ph.D. thesis, Univ. of Wis.-Madison, 351 pp., 1996.

Orsolini, Y. J., V. Limpasuvan, and C. B. Leovy, The tropical stratopause in the UKMO stratospheric analyses: Evidence for a 2-day wave and inertial circulations, *Q. J. R. Meteorol. Soc.*, *123*, 1707–1724, 1997.

O'Sullivan, D. J., and M. H. Hitchman, Inertial instability and Rossby wave breaking in a numerical model, *J. Atmos. Sci.*, *49*, 991–1002, 1992.

Reber, C. A., The Upper Atmosphere Research Satellite (UARS). *Geophys. Res. Lett.*, *20*, 1215–1218, 1993.

Roche, A. E., J. B. Kumer, J. L. Mergenthaler, G. A. Ely, W. G. Uplinger, J. F. Potter, T. C. James, and L. W. Sterritt, The cryogenic limb array etalon spectrometer (CLAES) on UARS: Experiment description and performance, *J. Geophys. Res.*, *98*, 10,763–10,775, 1993.

Russell, J. M., III, L. L. Gordley, J. H. Park, S. R. Drayson, W. D. Hesketh, R. J. Cicerone, A. F. Tuck, J. E. Frederick, J. E. Harries, and P. J. Crutzen, The Halogen Occultation Experiment, *J. Geophys. Res.*, *98*, 10,777–10,797, 1993.

Sassi, F., R. R. Garcia, and B. A. Boville, The stratopause semiannual oscillation in the NCAR community climate model, *J. Atmos. Sci.*, *50*, 3608–3624, 1993.

Shiotani, M., J. C. Gille, and A. E. Roche, Kelvin waves in the equatorial lower stratosphere as revealed by cryogenic limb array etalon spectrometer temperature data, *J. Geophys. Res.*, *102*, 26,131–26,140, 1997.

Swinbank, R., and A. O'Neill, A stratosphere-troposphere data assimilation system, *Mon. Weather Rev.*, *122*, 686–702, 1994a.

Swinbank, R., and A. O'Neill, Quasi-biennial and semi-annual oscillations in equatorial wind fields constructed by data assimilation, *Geophys. Res. Lett.*, *21*, 2099–2102, 1994b.

Watson, R. T., et al. (Eds.), Present state of knowledge of the upper atmosphere 1988: An assessment report, *NASA Ref. Publ.*, *1208*, 1988.

Winter, T., and G. Schmitz, On divergent barotropic and inertial instability in zonal-mean flow profiles, *J. Atmos. Sci.*, *55*, 758–776, 1998.

J. C. Gille, National Center for Atmospheric Research, P.O. Box 3000, Boulder, CO 80307.

H. Hayashi and M. Shiotani, Graduate School of Environmental Earth Science, Hokkaido University, Sapporo 060-0810, Japan. (e-mail: hiroo@ees.hokudai.ac.jp)

(Received January 19, 1998; revised May 6, 1998;
accepted May 11, 1998.)